

ARTICLE

Laurent Beney · Elodie Linares · Eric Ferret
Patrick Gervais

Influence of the shape of phospholipid vesicles on the measurement of their size by photon correlation spectroscopy

Received: 4 December 1997 / Revised version: 2 March 1998 / Accepted: 15 April 1998

Abstract The influence of shape transformation of large unilamellar vesicles (LUV) on their size measurement by photon correlation spectroscopy (PCS) has been investigated. The experimental size of vesicles after hyperosmotic contractions of increasing intensities have been compared to the theoretical volume decrease determined by applying Boyle Van't Hoff's law. The main observation is that PCS size measurement gives overestimated values when LUV have been subjected to a volume decrease of more than 20% of their initial volume. The PCS size overestimation is related to the influence of the shape transformation of the vesicles on their diffusion coefficient (D) as shown by modelling the evolution of D of a sphere which is transformed into an ellipsoid by internal volume reduction under constant area.

Key words Liposomes · Shape · Diffusion coefficient · Photon correlation spectroscopy

Introduction

Photon correlation spectroscopy (PCS) is a non-destructive procedure for measuring the size of particles in a suspension typically in the submicron region. PCS measures the Brownian motion and relates this to the size of the particles by applying the Stokes-Einstein equation, assuming particles to be spherical. In fact the measured diameter refers to how the particle moves within a fluid, i.e. the hydrodynamic diameter. The volume of liposomes is a determinant parameter that is required in order to determine their encapsulation capacity or the bilayer permeability parameters. PCS is routinely used to characterise the size of liposomes because it presents many advantages when com-

pared to other methods which require long preparation procedures, i.e. entrapment of labelled and fluorescent molecules, or methods which alter the suspension, i.e. electron microscopy.

Shape transitions of lipid vesicles are induced by variation of their area-to-volume ratio, transforming spherical vesicles into a wide variety of shapes which include ellipsoids, discocytes, stomatocytes or budded vesicles (Kas and Sackmann 1991). The extent of their deformation is related to the degree of increase in area-to-volume ratio and to other parameters such as the area difference between the inner and the outer monolayer (Mui et al. 1995) and in the case of vesicles composed of phospholipid mixtures, by additional factors such as the preferential distribution of components between the two monolayers, the different spontaneous curvatures of the lipids domains and the interfacial energy between the domains (Seifert 1993).

Changing the osmotic pressure is a means to modify the area-to-volume ratio of vesicles. Hyperosmotic perturbations lead to water exit from the vesicle lumen, which equilibrates the intra- and extra-vesicular osmotic pressures, and leads to a vesicle deformation because the bilayer area is almost constant during osmotic shrinkage.

Because PCS allows the size determination of particles which are assumed to be spherical and because vesicles may be subjected to shape transitions in conditions where their internal volume decreases, we propose here to study the influence of vesicle shape transformation on the measurement of vesicle size by means of PCS. The vesicle volume decrease and the corresponding deformation have been modulated by increasing the osmolarity of the medium with glucose. The experimental data have been compared to the theoretical volume of the LUV, determined by applying Boyle Van't Hoff's law.

Next, the previously shrunk vesicles were allowed to swell in a medium of solute concentration that was equal to the initial one (preparation medium). The size of the liposomes was again measured after this step in order to compare the vesicle size to the original one and hence to investigate any fusion or vesiculation phenomena which could influence the size measurement.

L. Beney · E. Linares · E. Ferret · P. Gervais (✉)
Laboratoire de Génie des Procédés Alimentaires
et Biotechnologiques,
Ecole Nationale Supérieure de Biologie Appliquée à l'Alimentation,
1 Esplanade Erasme, F-21000 Dijon, France
e-mail: gervais@satie.u-bourgogne.fr

Table 1 Hyperosmotic gradients of glucose applied to the vesicles and corresponding theoretical volumes of the vesicles after osmotic shrinkage (from Boyle Van't Hoff's law)

Liposome sample (in glucose 0.02 M)	Control	1	2	3	4	5	6	7	8
Hyperosmotic gradient of glucose (M)	0	0.002	0.004	0.006	0.008	0.01	0.014	0.018	0.02
Theoretical volume of the vesicles (% of initial volume)	100	90.9	83.3	76.9	71.4	66.7	58.8	52.6	50

Materials and methods

Materials

Egg yolk phosphatidylcholine (EYPC) and n-octylglucoside were purchased from Sigma (St. Louis, MO) and stored at -20°C under nitrogen.

Vesicles preparation

The liposomes prepared for this experiment were large unilamellar vesicles (LUV), which present the homogenous and monodisperse size distribution which is required for light-scattering experiments, and giant vesicles, intended for microscopic observation. For the preparation of LUV, we used the detergent dialysis method (Zumbuehl and Weder 1981) using the "Liposomat" (Dianorm Geräte, München, Germany). Phosphatidylcholine and n-octylglucoside at a molar ratio of 1:5 were dissolved in 10 ml chloroform at a final lipid concentration of 4 mg/ml. The solution was placed in a round bottomed flask and allowed to form a thin film after evaporation of the solvent under vacuum overnight. The dried lipid film was then hydrated with 20 ml of a 20 mM glucose solution to obtain a mixed lipid/detergent micelle solution. This was then recycled through the "Liposomat" dialyser for 12 hours which permitted slow removal of detergent by dialysis against 5000 ml of 20 mM glucose solution. The vesicle suspension was then filtered through a $0.4\ \mu\text{m}$ polycarbonate filter (Millipore Corporation, Bedford, USA).

Giant vesicles were prepared using a modification of the technique of Reeves and Dowben (1969) as described by Steponkus and Lynch (1989). The lipid was dissolved in chloroform:methanol (1:1 v/v) at a concentration of 0.96 mg/ml. The solution was drawn into glass capillary tubes (0.6 mm in diameter) and then expelled using a stream of nitrogen. After solvent evaporation for 24 hours, capillary tubes containing a thin film of phospholipids were filled with a 20 mM glucose solution saturated with nitrogen, sealed at one end and then allowed to equilibrate for 8 to 12 hours. Vesicles were collected in 20 mM glucose solution and used immediately after preparation.

Osmotic treatments

The osmolyte used to modify the volume of the vesicles is glucose because of the low permeability of phosphatidylcholine bilayers to this solute (Wood et al. 1968; Inoue

1974). Moreover, glucose is electrically neutral, and prevents the aggregation and/or fusion of liposomes during dehydration processes (Suzuki et al. 1996). For PCS measurements, LUV prepared in 0.02 M glucose were mixed with medium that was made hypertonic by varying the glucose concentration, in order to yield the osmotic gradient across the vesicle bilayer, described in Table 1. The final lipid concentration was identical and equal to 0.07 mg EYPC/ml in each sample. All PCS measurements of the osmotically treated liposomes were accomplished 30 minutes after mixing, and all solutions were systematically filtered in order to avoid dust contamination. The experiments were carried out at a temperature of 20°C .

The second step of the osmotic treatment consisted of placing the shrunken liposomes in a 0.02 M glucose solution (preparation medium). This treatment was accomplished by addition of distilled water to the hyperosmotic vesicle solutions, and by a further addition of isotonic glucose (0.02 M), to achieve the same dilution in each vesicle sample (0.005 mg EYPC/ml).

Theoretical volume of the shrunken liposomes

The theoretical volume decrease of the vesicles induced by the concentration increase of a non permeating solute in the external medium can be determined by applying Boyle Van't Hoff's law. The theoretical volume of the liposomes after the osmotic shocks was determined by assuming that the liposome volume decrease is the exclusive result of a water exit, which allows the intra- and extravesicular solute concentrations to equilibrate. This assumption was made because of the very low permeability of phosphatidylcholine bilayers to glucose. We have also considered that water exit from the liposomes does not modify the extracellular glucose concentration because the extra to intravesicular volume ratio is high. The increase in vesicle bending energy cause by deformation which can prevent a complete concentration equilibration was neglected. Thus, the calculated sizes were obtained by considering that the internal volume (V_i) and the internal osmotic pressure (Π_i) of the vesicle are related by the Boyle Van't Hoff expression:

$$\Pi_i = \frac{nRT}{V_i} \quad (1)$$

As Π_i is linearly related to the internal glucose concentration ($C_i = n/V_i$) in the concentration range considered in these experiments (water activity >0.99), the relation between the initial and the final volume of the vesicle, V_{i1}

and V_{i2} respectively, and the concentration gradient across the vesicle bilayer is:

$$C_{i1} \cdot V_{i1} = C_{i2} \cdot V_{i2} \quad (2)$$

where, C_{i1} is the initial and C_{i2} is the final glucose concentration of the medium. The theoretical volume decrease for each osmotic gradient is given in Table 1. The theoretical volumes of the vesicles for the different osmotic gradients that are proposed in Fig. 1 B are expressed as volumes relative to the initial one (100% in isotonic medium).

Microscopy

The diameter of the LUV produced by the dialysis method is typically 100–150 nm so the shape modification of the vesicles has been observed microscopically on giant vesicles suspended in solutions of increasing concentration following the same procedure as for LUV. Giant vesicles were observed with an inverted light microscope (Leitz, Wetzlar, Germany) equipped with an objective lens (FLUOTAR GF 25/0.35; Leitz, Germany). Microscopic observation could be instantaneously recorded via a 1/3' CCD camera (I2S, Pessac, France) on a microcomputer (Hewlett Packard, Sunny Vale, CA) through an image-grabbing system (MATROX, Dorval, Canada), previously described (Beney et al. 1997).

Photon correlation spectroscopy

The apparatus used is an Autosizer LoC (Malvern Instruments, Malvern, UK). Light from a 15 mW helium-neon Laser at 633 nm is focused onto the vesicle sample in a glass cuvette maintained at constant temperature ($20^\circ\text{C} \pm 0.1^\circ\text{C}$) by as Pelltier thermostat. Thermal equilibration time (5 min) was allowed after introduction of the sample and before the start of a measurement. The intensity of the scattered light is detected at 90° to the incident beam. Sample times of approximately 20 μs were employed. The experimental duration time was $300 \text{ s} \pm 20$. The correlation function was accumulated in a 64 channel photon autocorrelator divided into 4 subcorrelators, collected by a computer and subsequently analysed by CONTIN, the analysis technique developed by Provencher (1982). The average diffusion coefficient was calculated from 10 successive autocorrelation functions.

The radius of the vesicles in a sample is calculated from the correlation function which is derived from the temporal fluctuations of light scattered by particles in solution. In PCS, the second order correlation function $g^{(2)}(\tau)$ is measured according to the following expression:

$$g^{(2)}(\tau) = A[1 + \beta |g^{(1)}(\tau)|^2] \quad (3)$$

where A is the base line, β is an equipment related constant, and $g^{(1)}(\tau)$ is the normalised first-order autocorrelation function.

For particles that are in constant random thermal, or Brownian motion, the normalised first-order autocorrela-

tion function, $g^{(1)}(\tau)$ decays exponentially with the delay time, and also depends upon the scattering vector, q , and the particle-size distribution:

$$g^{(1)}(\tau) = \int_0^\infty F(\Gamma) \exp(-\Gamma\tau) d\Gamma \quad (4)$$

where $F(\Gamma)$ is the normalised distribution function of the decay constant Γ , $\Gamma = Dq^2$, $q = (4\pi n/\lambda) \sin(\theta/2)$, n is the refractive index of the medium, λ is the wavelength of incident light, θ is the scattering angle, and D is the particle diffusion coefficient.

In the method developed by Provencher (1982), the computer searches for the smoothest non-negative solution for $F(\Gamma)$ that is consistent with the experimental data. This method was chosen because it gives more consistent solutions, even for polydisperse particle samples. According to Eq. (4), the computer calculates the particle diffusion coefficient, D , which is related to the particle hydrodynamic radius (R_H) by the Stokes-Einstein relation:

$$R_H = \frac{kT}{6\pi\eta D} \quad (5)$$

where k is the Boltzmann's constant, η is the viscosity of the solution and T is the absolute temperature.

Refractive indices and viscosities of glucose solutions were determined using theoretical data (Weast et al. 1985). The light scattering apparatus was calibrated with a standard, monodisperse sample of polystyrene latex spheres (102 ± 3 nm in diameter) (Duke Scientific Corporation, Palo Alto, USA). Each measurement gave the mean value of a number distribution of vesicle diameters. Each experimental value presented in Fig. 1 A is the mean value of 10 measurements and the bars correspond to the standard deviation. The distribution width (width at half height of the distribution peak) did not change significantly upon increasing the osmotic gradient and was typically equal to 24 ± 3 nm.

The comparison between the theoretical and the experimental volumes has been accomplished by calculating the volume of a spherical particle from the experimental diameter, since PCS assumes particles to be spherical. The experimental volumes determined by this way have been related to the isotonic one and expressed as relative volumes (Fig. 1 B).

Results

Comparison between the experimental and theoretical LUV sizes

The theoretical and the experimental volume decrease of LUV after hyperosmotic shifts of increasing intensities, are presented in Fig. 1 B. Comparison of the experimental and theoretical curves shows that for a theoretical volume decrease to less than 20% of the initial volume, the experi-

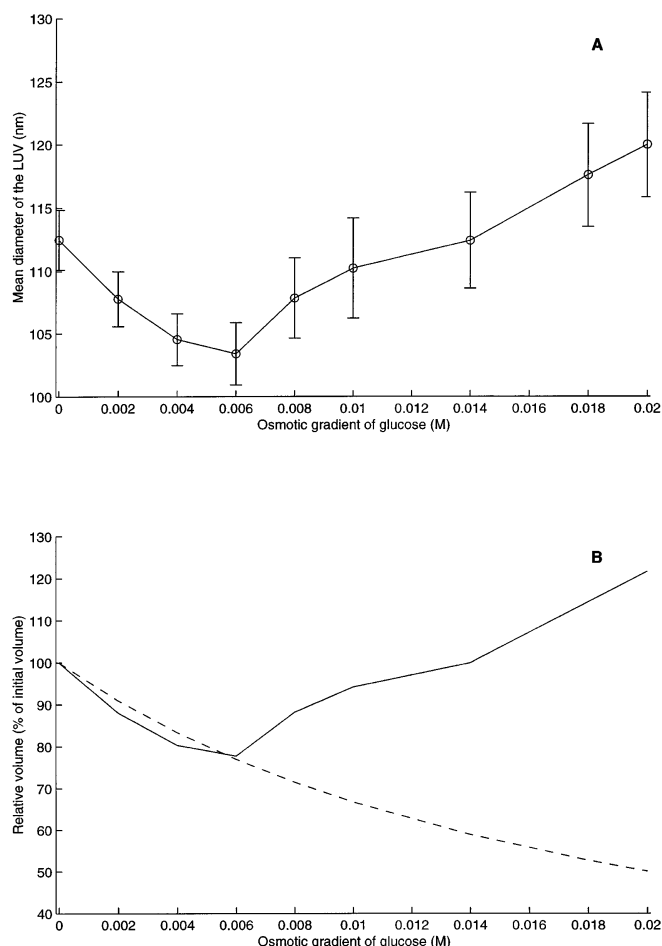


Fig. 1 **A** Experimental diameters of the LUV after hyperosmotic treatments of increasing gradients of glucose. **B** Theoretical (dotted line) and experimental volume decreases of the LUV after osmotic treatments of increasing gradients

mental and the theoretical volumes are the same, within error. However, for the case where the volume decrease is more than 20% of the initial volume, the volume of the LUV measured by means of PCS is overestimated when compared to the theoretical value. In fact, beyond this limit, the experimental diameter values increase progressively, with the osmotic increase amplitude, until the initial LUV size is again reached and then exceeded, i.e. the size determined experimentally for a theoretical 30% volume decrease is equal to the size of the LUV in their isotonic or preparation medium (Fig. 1A). In consequence, the difference between the theoretical and the experimental volumes increases with the osmotic increase amplitude from glucose gradients of 0.006 to 0.02 M.

The osmotically shrunken LUV have been placed in a medium of glucose concentration equal to the preparation one by water addition. No significant difference was found between the final size of LUV that have been subjected to an hyperosmotic contraction followed by re-swelling and osmotically untreated LUV (data not shown). This result demonstrates that LUV have not been subjected to fusion or fragmentation during the osmotic shrinkage, even for a

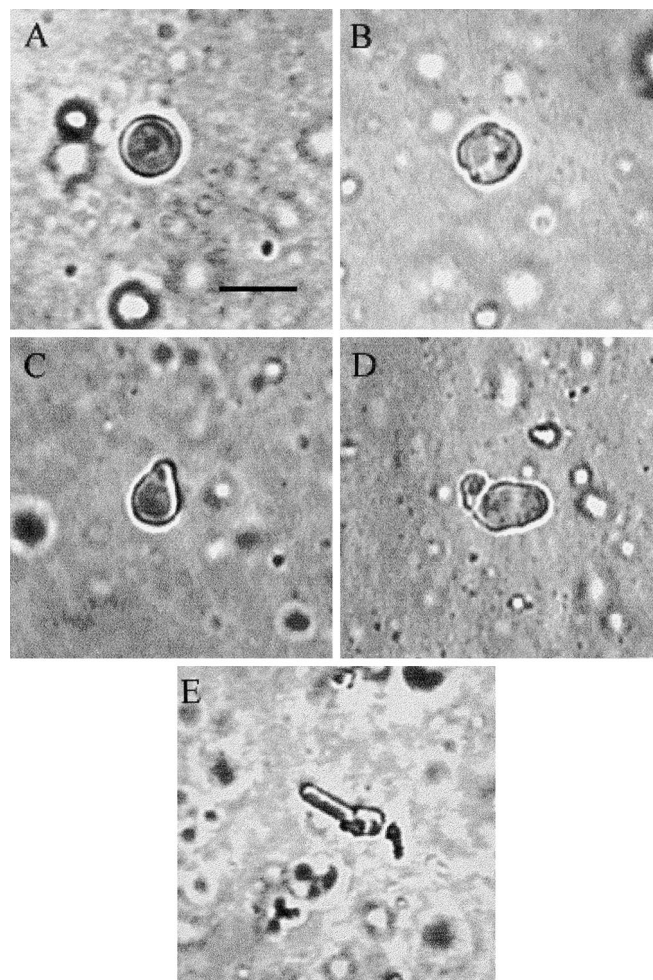


Fig. 2 **A–E** Morphology of the giant vesicles after volume reduction (VR) of increasing intensities. **A** vesicle in glucose 0.020 M (isotonic), VR=0%, the bar represents 5 μ m; **B** glucose 0.024 M, VR=16.7%; **C** glucose 0.026 M, VR=23.1%; **D** glucose 0.030 M, VR=33.3%; **E** glucose 0.040 M, VR=50.0%

volume decrease corresponding to 50% of the initial volume. It can also be concluded that the vesicles remain osmotically sensitive after shrinkage.

Morphological behaviour of the giant vesicles

The videomicrographs of giant vesicles osmotically treated in the same conditions as the LUV and as proposed in Table 1, are presented in Fig. 2. The extent of the shape modification of the liposomes, induced by the decrease in their internal volume while their bilayer area remains constant, increases with the amplitude of the osmotic shock. The vesicle shape that is initially spherical (Fig. 2A) becomes more complex with the level of osmotic shrinkage. The surface of the vesicles that have been subjected to a volume decrease which does not exceed 20% of the initial volume, are characterised by a slight deformation (Fig. 2B). For volume decreases of higher intensities the liposomes are subjected to drastic morphological changes which lead

to the formation of a bud (Fig. 2C), a vesicle-like structure (Fig. 2D) and finally to finger-like projection (Fig. 2E).

Discussion

Vesicle shape transformation

Considering that liposomes are subjected to a morphological transition which is closely related to the amplitude of the osmotic increase and that size measurement accomplished with PCS coincides with the theoretical volume decrease for volume decreases less than 20% of the initial volume, it appears that slight osmotic increases which induce slight shape modifications (Fig. 2A, and Fig. 2B) have negligible effects on PCS measurement accuracy. In the case of larger osmotic increases which cause more pronounced morphological changes, the size measurement of the liposomes by means of PCS becomes inappropriate. Since no fragmentation or fusion phenomena occurred during vesicle shrinkage, it appears that this limit corresponds, with regard to the shape of giant vesicles under increasing glucose gradients, to the level of volume contraction (for a constant area) which generates the appearance of vesicles on the liposome surface (Fig. 2C, Fig. 2D, and Fig. 2E). The morphological change we have observed correspond, according to Sackmann (1994), to the path of shape transition from the spherical to the pear shape, and then from pear to dumbbell shape. Even though the morphology of vesicles after osmotic shrinkage has been observed on giant vesicles we can suppose that LUV are similarly subjected to drastic shape changes. This assumption is supported by the fact that small unilamellar vesicles with diameters of approximately 20 nm also respond to salt gradients by a volume variation which in the case of hyperosmotic treatment produces shrinkage and collapse of initially spherical vesicles to flattened disks (Lerebours et al. 1993). According to the previous observations, the size overestimation of the shrunken vesicles by PCS is probably related to their shape modification and/or to a change in their optical properties. Concerning this last point, White et al. (1996) have recently demonstrated that phospholipid vesicle membranes, composed of dioleoyl phosphatidyl glycerol (DOPG), exhibit large optical changes in response to NaCl osmotic gradients. These changes are attributed to modifications of the refractive index of the bilayer caused by the alteration of hydration of the phospholipid headgroups, which influences the phospholipid packing density. The change in vesicle shape, arising from volume variation (from 0 to 25% volume decrease) was not found to influence the vesicle scattering properties (White et al. 1996). Our results show that the volume decrease of vesicles composed of egg yolk phosphatidyl choline, osmotically shrunk with glucose, is measurable with PCS in the volume decrease range 0–20%. This observation is not consistent with a change in the vesicles optical properties in this volume variation range, described by White et al. (1996). This divergence probably results from the differ-

ence in the nature of the osmotic solute and of the bilayer phospholipids, because White et al. (1996) have also shown that glycerol and betaine do not induce the large scattering changes of the DOPG vesicles observed with NaCl.

Shape transition modelling

As the vesicle geometrical transition of budding is characterised by an increase in vesicle eccentricity (see Eqs. (6a) and (6b)), the influence of this parameter on the PCS measurement has been theoretically investigated by calculating the variation of the diffusion coefficient of a particle of constant area which is initially spherical and then transformed into a prolate or an oblate ellipsoid by internal volume decrease. These model paths of shape transitions have been selected since the prolate one reproduces the increase in eccentricity of the shrunken vesicles we have observed and because small shrunken vesicles are also transformed into oblate ellipsoids (Lerebours et al. 1993). Theoretically, the oblate ellipsoid is a vesicle shape of low bending energy after a volume reduction of 50% and the prolate ellipsoid approaches the dumbbell shape which is another shape of low bending energy for an equivalent volume decrease (Seifert et al. 1991). Furthermore, the theoretical relation between the diffusion coefficient and the geometry of a particle is only available for a few shapes, which include discoids, rods and ellipsoids. Therefore, we have first determined the axis variation of a sphere, of initial diameter equal to the mean diameter of LUV in the isotonic medium (112 ± 2 nm), which is transformed into a prolate or an oblate ellipsoid by reduction of its internal volume. This step was accomplished by the determination of the revolution semiaxis (a) and equatorial semiaxis (b) of prolate and oblate ellipsoids of given volume (V) and area (A). A least square non-linear optimisation has been computed (Gauss-Newton method) on Matlab 5.1 (Math Works Inc., Natick, MA, USA) to solve the following equation systems which correspond to the area (A_{pro}) and the volume (V_{pro}) of a prolate ellipsoid:

$$\begin{aligned} V_{pro} &= \frac{4}{3}\pi \cdot a \cdot b^2 \\ A_{pro} &= 2\pi \left(b^2 + \frac{a \cdot b}{e_{pro}} \cdot \text{Arcsin } e_{pro} \right) \\ \text{with eccentricity } e_{pro} &= \left(1 - \frac{b^2}{a^2} \right)^{\frac{1}{2}} \end{aligned} \quad (6a)$$

and to the area (A_{obl}) and the volume (V_{obl}) of an oblate ellipsoid:

$$\begin{aligned} V_{obl} &= \frac{4}{3}\pi \cdot a \cdot b^2 \\ A_{obl} &= 2\pi \left(b^2 + \frac{a^2}{2 \cdot e_{obl}} \cdot \ln \frac{1 + e_{obl}}{1 - e_{obl}} \right) \\ \text{with eccentricity } e_{obl} &= \left(1 - \frac{a^2}{b^2} \right)^{\frac{1}{2}} \end{aligned} \quad (6b)$$

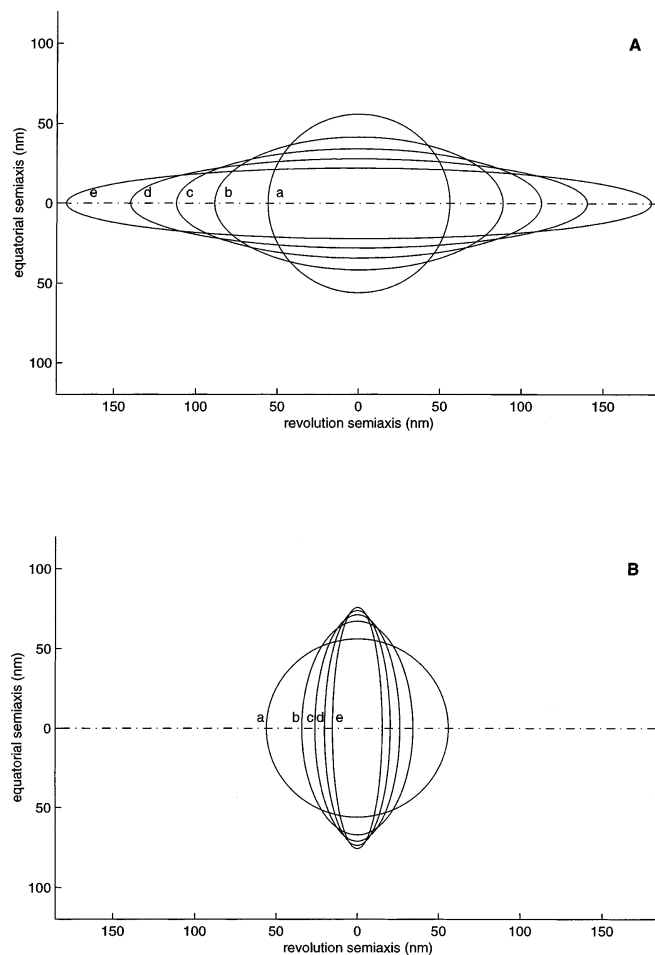


Fig. 3 **A** Shape evolution of a sphere transformed into a prolate ellipsoid by volume reduction and under constant area. **B** Shape evolution of a sphere transformed into an oblate ellipsoid by volume reduction and under constant area. The volume reduction (VR) of each ellipsoid is: (a): VR=0%, (b): VR=12.5%, (c): VR=25%, (d): VR=37.5%, (e): VR=50%

From the initial sphere ($radius = a = b = 56 \cdot 10^{-3} \mu m$, $area = A_i = 3.94 \cdot 10^{-2} \mu m^2$; $volume = V_i = 7.356 \cdot 10^{-4} \mu m^3$;) the volume V continuously decreases: $V = \alpha V_i$ with α ranging from 100% to 50%, and A remaining constant and equal to A_i . The semiaxes a and b are determined for each prolate and oblate ellipsoid (area A and volume αV_i) which are presented in Fig. 3A and Fig. 3B for prolate and oblate ellipsoids, respectively. The exact diffusion coefficients (D_{pro} and D_{obl}) corresponding to these ellipsoids are calculated by applying the following relations (from Perrin 1936):

for prolate ellipsoids

$$D_{pro} = \frac{k \cdot T}{6\pi\eta} \cdot \frac{1}{a \cdot e_{pro}} \cdot \ln \frac{a \cdot (1 + e_{pro})}{b} \quad (7a)$$

for oblate ellipsoids

$$D_{obl} = \frac{k \cdot T}{6\pi\eta} \cdot \frac{1}{a \cdot e_{obl}} \cdot \text{Arc tan} \frac{b \cdot e_{obl}}{b} \quad (7b)$$

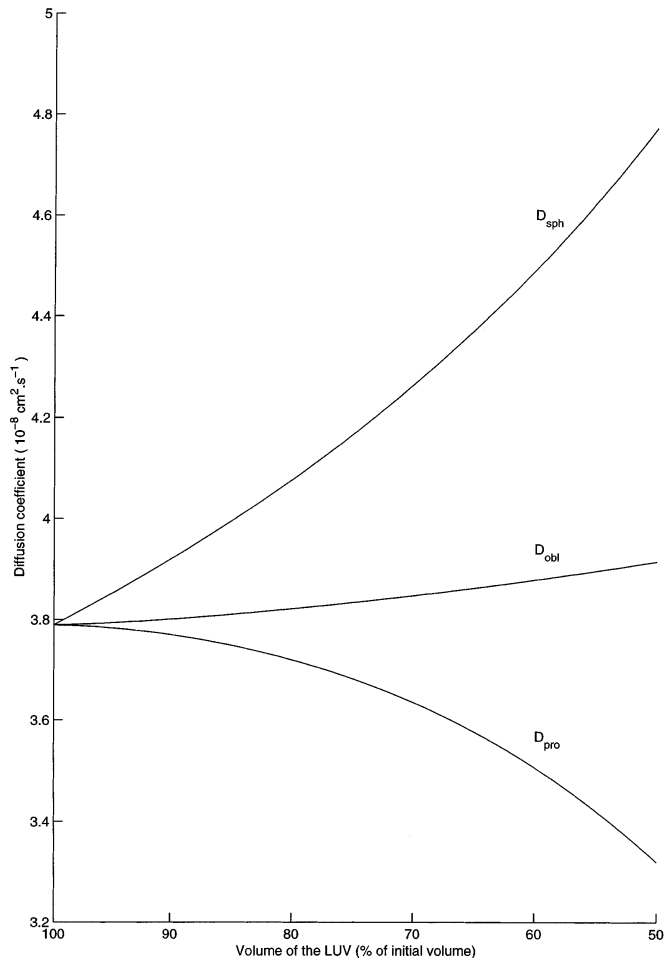
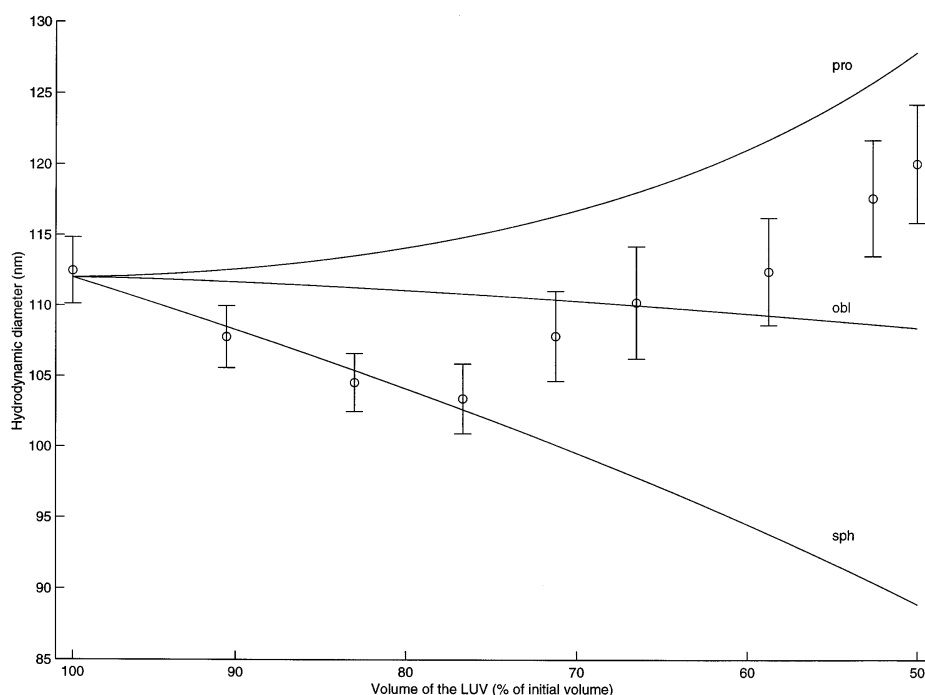


Fig. 4 Evolution of the diffusion coefficient of a sphere (D_{sph}) which remains spherical by decrease in area or which is transformed into a prolate (D_{pro}) and an oblate (D_{obl}) ellipsoid through volume decrease and under constant area

Figure 4 represents the variation of the diffusion coefficient of an initially spherical vesicle which is transformed into an oblate and a prolate ellipsoid vesicle by internal volume decrease and the diffusion coefficient (from Eq. (5)) of a sphere which is subjected to the same volume decrease but which remains spherical by area decrease. This curve shows that the diffusion coefficient of the prolate ellipsoid (D_{pro}) exponentially decreases with its deformation, whereas the diffusion coefficient of the sphere (D_{sph}) exponentially increases with its volume decrease. D_{obl} is subjected to a slight increase in this range of volume variation. In consequence, D_{sph} is always higher than D_{pro} and D_{obl} for the same volume. The difference between the diffusion coefficients of the sphere and the ellipsoids increases with the level of the volume reduction and is mainly related to the increase in eccentricity caused by the volume reduction of the ellipsoids and to the radius decrease of the sphere. From Eq. (5), we can conclude that the hydrodynamic radius, calculated from D_{pro} , of an initially spherical particle which is transformed into a prolate ellipsoid when it is subjected to a volume decrease and assumed

Fig. 5 LUV diameters measured by PCS (○) for volume reductions ranging from 0 to 50% and LUV modelled diameters. Assuming that vesicles are transformed into prolate (*pro*) and oblate (*obl*) ellipsoids of increasing eccentricity through volume reduction. Assuming that vesicles remain spherical by area decrease (*sph*)



to be spherical, as in PCS, increases with its volume decrease. Under the same conditions, the hydrodynamic radius of a spherical particle which is transformed into an oblate ellipsoid is subjected to a slight decrease with its volume decrease. The experimental diameters of the LUV under increasing osmotic gradients are compared in Fig. 5 with the values calculated with the prolate and oblate models and with the values determined by considering that LUV remain spherical. The experimental values are contained between the spherical and the prolate values. From 100 to 75% of their initial volume the experimental diameters follow the spherical model. From 75 to 60% of their initial volume the experimental values reach the oblate values and are, for higher volume decrease, contained between the oblate and the prolate values. It should be remarked that the experimental values never reach the prolate values. The influence of the shape transformation of the vesicles, by their increase in eccentricity, on their Brownian coefficient is consistent with the LUV size overestimation measured by PCS. However, the ellipsoidal models are inappropriate for volume decreases ranging from 0 to 20% of the LUV's initial volume. This could be explained by the lack of minimum bending energy constraint in the ellipsoidal models which induces high deformations for small volume decreases whereas giant vesicles (Fig. 2A and Fig. 2B) are almost spherical after volume decreases ranging from 0 to 20% of their initial volume. The effect of the lack of minimum bending energy constraint in the ellipsoidal models is illustrated by the difference between the shape of the giant vesicle presented in Fig. 2B and the ellipsoids noted (b) in Fig. 3A and Fig. 3B. These shapes are the experimental (Fig. 2B) and modelled deformations (Fig. 3A and Fig. 3B) corresponding to volume reductions

of 16.7 and 12.5%, respectively. The decrease in diameter detected by PCS up to an osmotic gradient of 0.006 M which coincide with the spherical model (decrease in area) can not be interpreted by a bilayer compression which is known to be limited. The lack of theoretical knowledge about the hydrodynamic diffusion coefficients of intermediate shapes such as pear shapes or budded forms limit our interpretations of the measurements accomplished up to this osmotic gradient. As the influence of the shape transformation of a spherical vesicle into a prolate or an oblate ellipsoid on its Brownian coefficient can explain the PCS size overestimation, and as phospholipid vesicles are subjected to drastic shape changes, which increase their eccentricity in response to many physical modifications of the environment, we conclude that this parameter needs to be considered when the size of phospholipid vesicles is determined with PCS, or dynamic light scattering.

This study has been carried out in order to investigate the shape effects of liposomes on their size measurement by means of PCS. The main conclusion is that PCS measurement is possible if the vesicle shape is approaching spherical and provided that no optical change occurs in the bilayer (White et al. 1996), but it gives an overestimated size for vesiculated liposomes. Therefore, special care must be taken if vesicles to be measured have been exposed to physical or chemical conditions that can modify the area to volume ratio of the vesicle, i.e. temperature, osmotic pressure (Sackmann 1994) or hydrostatic pressure (Beney et al. 1997), or which modify the difference in area between the two monolayers, i.e. pH gradient, chemical agents or extrusion process (Mui et al. 1993; Mui et al. 1995).

References

- Beney L, Perrier-Cornet JM, Hayer M, Gervais P (1997) Shape modification of phospholipid vesicles induced by high pressure: influence of bilayer compressibility. *Biophys J* 72:1258–1263
- Inoue K (1974) Permeability properties of liposomes prepared from dipalmitoyllecithin, egg lecithin, rat liver lecithin and beef brain spingomyelin. *Biochim Biophys Acta* 339:390–402
- Kas J, Sackmann E (1991) Shape transitions and shape stability of giant phospholipid vesicles in pure water induced by area-to-volume changes. *Biophys J* 60:825–844
- Lerebours B, Wehrli E, Hauser H (1993) Thermodynamic stability and osmotic sensitivity of small unilamellar phosphatidylcholine vesicles. *Biochim Biophys Acta* 1152:49–60
- Mui BL-S, Cullis PR, Evans EA, Madden TD (1993) Osmotic properties of large unilamellar vesicles prepared by extrusion. *Biophys J* 64:443–453
- Mui BL-S, Döbereiner HG, Madden TD, Cullis PR (1995) Influence of transbilayer area asymmetry on the morphology of large unilamellar vesicles. *Biophys J* 69:930–941
- Perrin F (1936) Mouvement brownien d'un ellipsoïde. II. Rotation libre et depolarisation des fluorescences. Translation et diffusion des molécules ellipsoïdales. *J Phys Radium* 7:1–11
- Provencher SW (1982) CONTIN, users manual. EMBL technical report DAO5. Heidelberg, European Molecular Biology Lab
- Reeves JP, Dowben RM (1969) Formation and properties of thin-walled phospholipid vesicles. *J Cell Physiol* 73:49–60
- Sackmann E (1994) Membrane bending energy concept of vesicle- and cell-shapes and shape-transitions *FEBS Lett* 346:3–16
- Seifert U, Berndl K, Lipowsky R (1991) Shape transformations of vesicles: phase diagram for spontaneous-curvature and bilayer-coupling models. *Phys Rev A* 44:1182–1202
- Seifert U (1993) Curvature-induced lateral phase segregation in two-component vesicles. *Phys Rev Lett* 70:1335–1338
- Steponkus PL, Lynch DV (1989) The behavior of large unilamellar vesicles of rye plasma membrane lipids during freeze/thaw-induced osmotic excursions. *Cryo Lett* 10:43–50
- Suzuki T, Komatsu H, Miyajima K (1996) Effects of glucose and its oligomers on the stability of freeze-dried liposomes. *Biochim Biophys Acta* 1278:176–182
- Weast RC, Astle MJ, Beyer WH (1985) Handbook of chemistry and physics. 66th edition. CRC Press, Boca Raton
- White G, Pencer J, Nickel BG, Wood JM, Hallett FR (1996) Optical change in unilamellar vesicles experiencing osmotic stress. *Biophys J* 71:2701–2715
- Wood RE, Wirth FP, Morgan HE (1968) Glucose permeability of lipid bilayer membranes. *Biochim Biophys Acta* 163:171–178
- Zumbuehl O, Weder HG (1981) Liposomes of controllable size in the range of 40 to 180 nm by defined dialysis of lipid/detergent mixed micelles. *Biochim Biophys Acta* 640:252–262